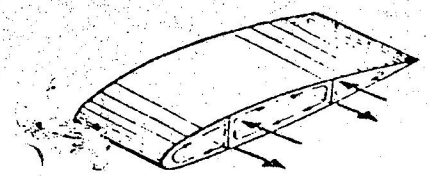

FANASA

FABRICA NACIONAL DE AEROPLANOS S. A.
OFICINA CENTRAL - APARTADO 5599
LIMA - PERU

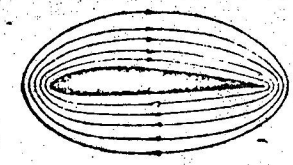

Quille		

ESTIMATION OF AERODYNAMIC LOADS

FOR STRUCTURAL DESIGN OF AN INVERTING FLAP

A COURTESY TRANSLATION BASED ON A

FANASA REPORT ACS-1 ENTITLED

"ESTIMADO DE LAS CARGAS AERODINAMICAS PARA

DISEÑO ESTRUCTURAL DE UNA ALETA INVERTIBLE"

ORIGINAL REPORT WRITTEN BY

PROFESOR ALBERTO ALVAREZ-CALDERON F. FROM

UNIVERSIDAD NACIONAL DE INGENIERIA

LIMA -- PERU

This report translation is sent by FANASA

to BRISTOL - WINNIPEG on OCT-22-1965

FABRICA NACIONAL DE AEROPLANOS S. A.
OFICINA CENTRAL · APARTADO 5599
LIMA · PERU

Translation ACS-1

TABLE OF CONTENTS

FANASA

FABRICA NACIONAL DE AEROPLANOS S. A.
OFICINA CENTRAL · APARTADO 5599
LIMA · PERU

Quill	Translation ACS-1	

Page Nº

List and copy of NACA figures of reference in this report

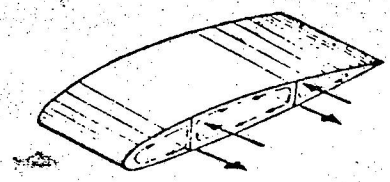

FANASA

FABRICA NACIONAL DE AEROPLANOS S. A.
OFICINA CENTRAL - APARTADO 5599
LIMA - PERU

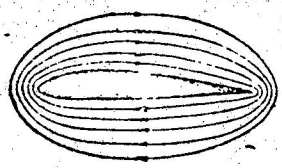

Mac		

ESTIMATION OF AERODYNAMIC LOADS FOR STRUCTURAL DESIGN OF AN INVERTING FLAP

ABSTRACT

The aerodynamic load that can be developed by an inverting flap having a chord of approximately 20% of the wing's chord have been examined for structural design purposes throughout the entire range of flap deflections.

Published tunnel data of other flaps have been used to estimate the loads of the inverting flap for the range $0° < \delta f < 90°$.

Reasonable assumptions related to published test data have been used to estimate loads for the deflection range of $\delta f > 90°$.

The aerodynamic loads for structural design of an inverting flap as determined by this report for a specific flap panel having an average flap chord of 1.65 feet and a flap span of 9.67 feet are, at 160MPH: 1965 pounds at 30° deflection with an approximately triangular chordwise flap pressure distribution, and 1300 pounds at 90° deflection with an approximately rectangular chordwise flap pressure distribution. At 120MPH, the loads per panel are 1105 pounds and 731 pounds at 30° and 90° flap deflection respectively.

With a properly designed flap support system, no flap buffet is encountered.

Maximum wing pitching moments due to flap occur at the 30° flap deflection.

No revesal of pitching moments are encountered in the inverted deflection range.

1. Introduction

The inverting flap system is described in U.S. patent 3.126.173. It is sketched in our Fig. 1. The geometric description of the flap is available in separate drawings. No wind tunnel data measuring flap loads exists for this type of flap. For structural design purposes, aerodynamic loads will be derived from published flap load data of other types of flaps for conventional flap deflections, and from reasonable assumptions for the remaining flap deflections.

2. Nature of aerodynamic flows and main sources of load data

The inverting flap system can be considered to develop loads under three different ranges of angular flap deflections δf, corresponding to the type of aerodynamic flows illustrated in our Figs. 2 as follows:

2.1

Our Fig. 2a. shows the attached flow field range, applicable for $10° < \delta f < 30°$,

the angles being measured in a conventional manner. For this range, Fowler flap type loads of NACA TR 620 will be assumed applicable.

2.2

Our Fig. 2b shows separated flap flows for the conventional defleation range of $30^{\circ} < \delta_f \leq 90^{\circ}$. For this range, the data of Fig. 24 and others of NACA TR 633 will be assumed applicable.

2.3

Our Fig. 2c shows separated flows existing for the inverted deflection range of $90^{\circ} < \delta_f \leq 170^{\circ}$. For this range, reasonable assumptions and experimental data related to Fig. 24 of NACA TR 633 will be used.

2.4

The special case of negative wing angles of attack and small flap deflections is discussed separately with reference to Fig. 35 of NACA TN 690.

3. Approximations of method, and review of wing pitching moments

In this section there will be reviewed the effect of variations in the flap crossectional shape, slot gap, flap chordwise position, flap chord, and wing section, on the estimation of inverting flap loads, and some wing loads, from published NACA data for other flaps, according to the methods described in paragraph 2 above.

3.1 Flap crossectional shape

Flap crossection of the inverting flap design corresponds to the NACA 23000 series from its rounded spanwise edge to approximately 30% of its chord, as specified in separate drawings. As seen in the extended position, its upper flap surface is straight to the thin spanwise edge of the flap; its lower surface is slightly convex. Consequently, the inverting flap has less camber than that had by the flap of the previously referred NACA test data, most of which have NACA 23000 series crossection.

In the attached flow range, for any given geometric flap deflection, the inverting flap with its smaller effective camber can develop flap loads no greater than those of the NACA flaps of NACA references. Therefore the use of the NACA references is structurally conservative with respect to differences in crossection and total[1] flap load developed for a given deflection.
In the separated flow regime, the crossection of the flap looses its importance in the determination of the flap loads. Consequently, the use of plain flap data for this range is thought acceptable, in particular in view of the flap gap comments of the following paragraph.

3.2 Flap gap

For the attached flow range of deflection the differences of gap size will be

assumed not to change the fundamental type of flap load magnitude and chordwise distribution, because the flow is attached in this range.

For the separated flow regime the gap between the flap and the wing which exists in the inverting flap does not act as a conventional high lift slot, but decreases the flap loads as is shown in our Fig. 3 based on Fig. 2 of NACA TN 650. Consequently, structural loads based on Fig. 24 of NACA TR 633 which does not have a slot gap, are structurally conservative when applied to inverting flap structural design in the pertinent separated flow range, as is explained later.

3.3 Flap chordwise position and wing pitching moments due to flap loads

Though wing pitching moments are not needed to design the flap's structure it is advantageous to review them. To estimate the effect of the chordwise position of the flap's "knee" on wing torsional loads due to flap loads it is necessary to determine how the inverting flap acts aerodynamically.

In the attached flow range, the inverting flap acts as a Fowler type flap, and its quarter chord pitching moments can be estimated from Fig. 10 of NACA TR 664 corresponding to an 0.26C Fowler flap with an NACA 23012 section. This assumption is conservative in that for a given geometric flap deflection, the inverting flap which has less flap camber than that of TR 664, cannot develop wing pitching movements greater than those in Fig. 10 of TR 664.

In the separated flow regime from our Fig. 2 it is evident the inverting flap, for $30^\circ < \delta_f < 90^\circ$, is similar to a plain flap in geometric flap disposition. Aerodynamically it could be thought to act, with respect to pitching moments (but not lift), and as a first approximation, as a plain flap also. With these assumptions, as a first approximation it could be thought that the inverting flap would develop, at certain deflections, quarter-chord section pitching moments similar to some of the values illustrated in our Fig. 4 which are taken from Figs. 11 and 9 of NACA TR 664, pertaining respectively to a Fowler type flap and a plain type flap. From our Fig. 4, it is evident that the maximum wing pitching moments occur for the Fowler flap at 30° deflection and are several times larger than those of the plain flap. The Fowler flap however, has a chord of 0.267C, and the plain flap has a chord of 0.20C. Furthermore, the inverting flap has its flap joint not at the 80% of the wing chord as had by the plain flap of our Fig. 4, but at 96% of the wing chord as sketched on our Fig. 1. Consequently, to apply the moments of our Fig. 4 to the inverting flap, certain corrections must be made.

The Fowler flap moment is proportional to the flap force which depends on the flap chord. Thus the Fowler data will be reduced by the factor $\frac{0.200}{0.267} = 0.75$ to represent the inverting flap under study. The actual inverting flap chord is 0.18C, so the factor 0.75 is conservative.

The plain flap moments are proportional to the distance between the flap joint and the aerodynamic axis flaps-up. This distance is 0.80C - 0.24C = 0.56C for the plain flap of Fig. 4; it is 0.96C-0.24C = 0.72C for the inverting flap. Con-

sequently the plain flap moments of our Fig. 4 must be increased by a factor of $\frac{.72}{.56}$=1.285 to represent the moments of an inverting flap.

With these considerations in mind, and using the above corrections, there is constructed Fig. 7 showing maximum Cm_{ac} vs δ_f, not necessarily at the same lift coefficient, for a 0.20C Fowler, and for a 0.20C "plain" flap with the flap knee at 0.96C. Fig. 7 was drawn from the following table:

Flap deflection Ref.Figs.3 & 10 NACA TR 664	(1) Cm_{ac} Fowler C_f=0.27C	(2) C_l OF(1)	(3) 0.75(1) C_f = 0.20C	(4) Cm_{ac} plain C_f=0.20C	(5) Cm_{ac} invert 1.285(2)	(6) C_l OF(4)
0°	- 0.17	2.0	0.127			
10°	- 0.33	2.2	0.248	-0.1	-0.1285	0.4
20°	- 0.48	2.4	0.36	-0.18	-0.232	0.4
30°	- 0.61	2.4	0.456	-0.19	-0.244	0.4
40°	- 0.45	1.6	0.337			
45°				-0.23	-0.296	0.4
60°				-0.25	-0.322	0.4
75°				-0.24	-0.309	0.4

In our Fig. 7, there is indicated in heavy dark lines the estimated pitching moments for the inverting flap.

It is evident by inspection that the maximum pitching moments occur for 30° inverting flap deflection, and that the Cm_{ac} for this condition is -0.456. The approximate vector representation is shown in our Fig. 6. (Advantage on trim: C_l at 90 C_l at 30; hence plane need not be flown with steady S_f with section C_m 0.32) Pitching moments for value of $\delta_f > 90°$ are thought smaller than those at 75° deflection because the flap load vector is acting close to the aerodynamic axis for the δ_f 90° range, as may be evident from our Fig. 5, and because the flap load vector may be even above the aerodynamic axis for $\delta_f > 90°$, as is sketched in our Fig. 9.

It could be considered from our Fig. 9 that for inverted flap deflections $S_f > 90°$, the flap loads act downward, to provide a pitch-up couple which might create a pitch reversal. While it is true that the flap loads act downward for this range it is also true that the added pressure in top of the flap manifests itself also on the lower surface of the wing above the flap, creating a local upward force ΔP on the wing's lower surface which tends to cancel the downward force on the flap. No pitch reversal should occur for $\delta_f > 90°$. A lack of aircraft pitch up for $\delta_f > 90°$ has been verified in flight tests.

3.4 Flap chord

The flap chord of most of the NACA data of reference in this report is either 20% or 26.7% of the wing's chord. The inverting flap under consideration for structural design has a flap chord of approximately 18% of the wing's chord. In this

report the test data for 20% chord flap will be applied directly to the 18% chord flap, which is structurally conservative and expedient. The existing test data on the 26.7% chord flap will be applied to the inverting flap corrected by a factor of $\frac{200}{267}$ when used for moments only.(2)

3.5 Wing thickness

The tests of reference in this report were made on an NACA 23012 airfoil. The wing on which the inverted flap will be tested is tapered and has a wing thickness varying from about 15% to about 20% on the flapped portion of the wing. Its airfoil section is from the NACA 23000 family.

Wing thickness is known to alter pressure magnitudes and distributions of a wing; it is thought to have very small influence on flap loads.

The only test data available for the purposes of this report is that of the NACA 23012 airfoil; no corrections have been applied for the flap loads to account for varying wing thickness.

4. Selection of flap deflections and loads for structural design of flap

4.1 Attached flow regime

From the Fowler flap data of NACA TR 620, the deflection with maximum flap loads corresponds to 30° and attached flows. It is shown in Fig. 8 of that report for a wing angle of attack α_o range of $-4.2° < \alpha_o < 1.7°$. It will be approximated for structural purposes as indicated below:

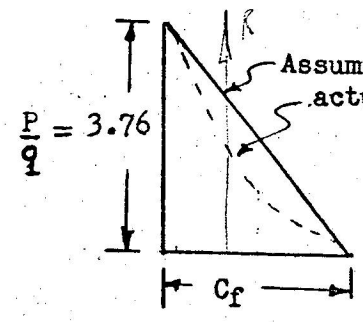

$$F \approx \frac{3.76 \times C_f}{2} \approx 1.9\, C_f$$

@ $-4.2 < \alpha_o < 1.70$; $\delta_f = 30°$

The assumed resulting force acts at one third of the flap's chord C_f.

It is noted that maximum wing loads occur for $\alpha_o = 8°$, accompanied by smaller flap loads.

This data is conservative to the extent that, for a given geometric flap deflection, the inverting flap which has less camber than the flap of TR 620, must develop slightly lower flap loads. It is also conservative in that the triangular distribution assumed includes more area than the actual distribution, and in that the resultant force acts more rearward than in the actual case (this vector location is also conservative with respect to retracting cable tension).

4.2 Separated flow regime, $30° < \delta_f < 90°$

The data for a plain flap in NACA TR 633 will be used for this purpose. From an examination of the loads for various deflections, which only cover up to 75°, it is evident that the 75° deflection yields largest flap loads.

One case of interest, by inspection of Fig. 24, is that of wing stall at α_o=16°. The flap load, approximated for structural purposes is represented below:

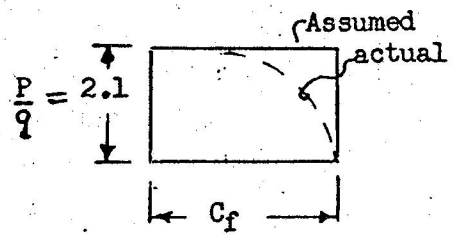

$F \sim 2.1 \times C_f$

@ α_o=16°, wing stalled, δ_f=75°

It should be realized that flight with a 75° flap deflection and with a stalled 16° wing angle of attack cannot normally be realized on an aircraft at maximum flap structural speed. It is apropriate, therefore, to consider[3] more realistic cases. There has been examined the loads for 75° flap deflection from $-12° \leq \alpha_o \leq 12°$; the critical load distributions within this range appears in the $-8 \leq \alpha_o \leq 8°$ and is assumed as indicated below:

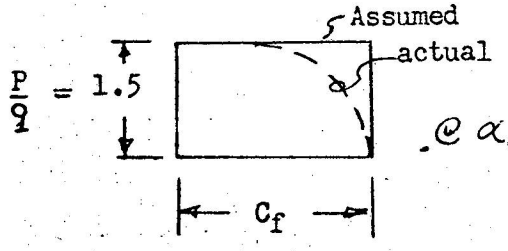

$F \sim 1.5 \times C_f$

@ α_o: $-8° < \alpha_o < 8°$, no gap

δ_f = 75°

The assumed resultant force acts at one half of the flap's chord C_f.

It is noted that maximum wing loads occur at α_o=12° which has smaller flap loads than the assumed case. The load above is too conservative for 75° deflection in that the assumed distribution includes more area than the actual one, and has a more rearward resultant force location than in fact. It is also too conservative in that it does not include the alleviating effect of the slot gap present in the inverting flap. These factors will be considered later.

The discussion so far has applied to 75° deflection of a plain flap without a slot. We now consider the alleviation of a slot.

The 75° load must be reduced by a factor taking into account the alleviating effect of the top gap of the inverting flap. This effect of the gap, which evacuates the high pressure region ahead of the flap, can be estimated conservatively at a wing angle of attack of 0°, since at this angle of attack nearly the entire change of drag force can be attributed to change of flap force. This change of drag force is presented in our Fig. 3. Assuming a flap gap of 3% of the wing chord for the 60° deflection, the correcting factor to account for the allevia-

ting effect of the slot on the flap is

$$\frac{C_{d_{o_{60^\circ}}} \text{ 0.03C Gap}}{C_{d_{o_{60^\circ}}} \text{ No Gap}} = \frac{0.238}{0.270} = 0.872$$

There is no reason why this alleviating effect measured at 60° should not be fully realized at 75° , or at 90° flap deflection. Consequently, the flap load at 75° is reduced by the above drag factor to be 1.5 (0.872) = 1.31 as shown below:

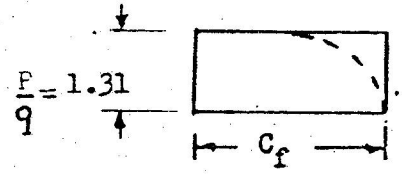

$F \sim 1.31\, C_f$

@ $-8^\circ < \alpha_o < 8^\circ$; 0.03C gap

$\delta_f = 75^\circ$

We now must estimate the flap loads at 90° deflection from the 75° data, since no pressure distribution exists for a 90° plain flap. Consider the wing drag measurements f or 0.20C 75° and 90° split flaps on a NACA 23012 airfoil, published in Fig. 8 of NACA TR 668. For the purposes of this report, the magnitude of the 75° flap load previously calculated will be used to estimate the 90° load assuming that it can be increased by the ratio of section drag coefficients of the NACA 23012 airfoil with 90° and with 75° flap deflection at a wing angle of attack of the order of 0°. This ratio is from TR 668, as follows:

FOR .10C SPLIT FLAP, NOT .20C

.20C split flap

$$\frac{C_{d_{o_{90^\circ}}}}{C_{d_{o_{75^\circ}}}} = \frac{1.15}{1.04} = 1.103 \qquad \frac{.215}{.176} = 1.22 = \frac{C_{d_{o_{75^\circ}}}}{C_{d_{o_{60^\circ}}}}$$

The use of the above ratio to predict the increase of flap load is thought reasonable in that the additional section drag at wing angles of attack of the order of 0° due to increasing flap deflection from 75° to 90° must appear principally as a flap force.

The estimated flap load for 90° deflection is then that estimated for 75° with a slot gap, corrected by an angle factor of 1.103, that is (1.31) (1.103) = 1.45, as shown below:

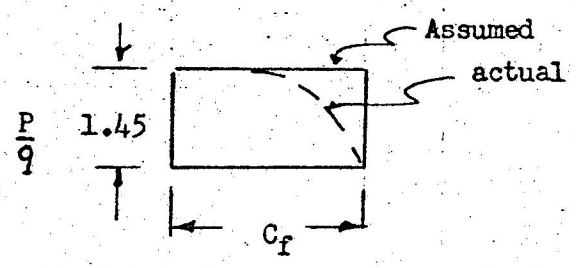

$F \sim 1.45\ C_f$

@ $8° < \alpha_o < 8°$; 0.03 c gap

$\delta_f = 90°$

The above assumed load for 90° is still too conservative in that the assumed distribution covers more area, and has a more reward location of its resultant force.than the actual distribution at 90°. Correction for actual load distribution is a graphical process deferred to a latter part of this report.

4.3 Separated flow regime, $90° < \delta_f \lesssim 170°$

No flap pressure distribution is known to this writer for this range of flap deflection. The fundamental type of flow is fully separated at the flap as sketched in our Fig. 2C. It is no different in kind from the separated flow for smaller flap deflections.

The 90° angle has been discussed previously in section 4.2. In this section the angles greater than 90° are in question. One specific question is: can there be any greater drag force than with 90° flap ?. The answer is evidently no, if 90° offers maxim effective frontal area with separated flow. Another question is: for δ_f greater than 90°, can there be flap loads greater than those at 90° ?. Consider the following: The flap load is determined by a positive pressure contribution in the front of the flap, and by a negative pressure contribution at its rear. The positive pressures contributions for $\delta_f > 90°$ stems from the destruction of kinetic energy, and for $S_f > 90°$ should not be thought any greater than with 90° flap. The negative pressures at the rear of the flap for $\delta_f > 90°$ are intimately related to the nature of the flow at the rear of the flap. This flow though difficult to predict is of the same type as that existing for 75° and 90° flap, namely, separated flap flow of the kind sketched in Figs. 2b and 2c, with local pressures probably somewhat below atmospheric, but without high negative values or peacks.

It is considered reasonable, and expedient, to assume for structural design purposes at $\delta_f > 90°$, that the flap load will not exceed that estimated for 90°. This is thought not unconservative to the extent that the flap is becoming less effective in producing drag forces for $\delta_f > 90°$, and the flow remains separated.

It is further pointed out that no flow mechanism can be envisioned, even as a possible but improbable flow, which may serve as a basis to question the above assumption regarding flap loads at $\delta_f > 90°$.

4.4 Small flap deflections and negative wing angles of attack

The flap actuator system is such that the flap is extended by spring loads and normally also by aerodynamic loads. For certain cases the flap loads could be

from Section 4.1:

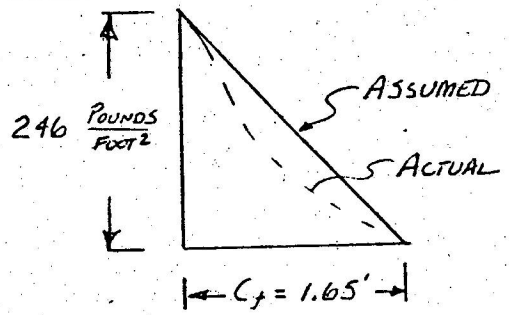

With the assumed load distribution, and an average flap chord of 1.65 feet, the flap load would be $\frac{246 \times 1.65}{2} = 202.5$ pounds per foot of span. With a flap span of 9.67 feet, the total load would be 1965 pounds per flap at 160MPH.

The assumed triangular load distribution has not been reduced to the smaller actual load distribution because the latter is not known with any reasonable certainty. The resultant force of the triangular distribution acts at the third of the flap's chord. These two load conditions are therefore structurally conservative.

6.2

The maximum flap load for the separated flow regime is from Sections 4.2 and 4.3.

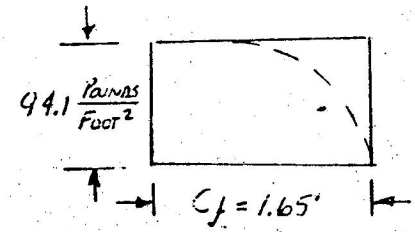

Assuming a rectangular pressure distribution and an average flap chord of 1.65 feet, the flap load would be (94.1) (1.65) = 155 LB_S per foot of flap span.

Before calculating the flap load, it is noted that the actual flap chordwise pressure distribution is not rectangular, but actually tapers off near the trailing edge as shown in NACA TN 633, Fig. 24. To avoid a pressure discontinuity a correction is therefore introduced to the above load per foot of flap span. This correction is calculated as the ratio of the graphic integration of the areas below the actual and rectangular load curves shown in our Fig. 9, and its numerical value is 0.865.

Taking into account a flap span of 9.65 feet, the total flap load is then (155) (0.865) (9.65) = 1300 pounds per flap at 160MPH. It is considered that, in view of the magnitude and shape of the pressure distribution in Section 6.1, it is both expedient and permissible to assume that the load of 1300 pounds calculated in this paragraph has actually a rectangular distribution. The resulting force vector acts at one half of the flap's chord, which is structuraly conservative for flap torsion and for the loads in the retraction system.

thought as capable of becoming negative i.e. act against the spring. This condition, which could exist, say, with severe negative gusts in take-off flaps, should be investigated. Fortunately, data is available in Fig. 35 of NACA TR 690 which, by inspection, is substantially applicable to the case in question, namely an inverting flap at small flap deflections. From that Fig. 35, it is seen that for flap deflections of 10°, i.e. approximately parallel and to the rear of the upper wing surface, and smaller than a normal take-off flap setting, it is not possible to develop negative flap loads prior to inverted wing stall, a condition normally not encountered in normal flight.

It is noted from Fig. 35 that for 0° flap deflection, negative flap loads could be developed which, if they overcame the sping loads, would deflect the flap downwards towards to a zero flap load position probably at around 5° for usual wing normal-force coefficients. It is evident from Fig. 35, that a stable flap position exists with no net flap load. The existence of such a position is, of course, well known from the stable position assumed by a stick-free control surface in flight. In the event of a failure of the inverting flap mechanism which would release completely the flap, it is evident from Fig. 35 that the flap would seek and assume a stable zero-flap-load position trailing the wing.

5. Flap structural speed

The aircraft on which the inverting flap will be tested has a maximum flap structural speed of approximately 120MPH.

The objective of the tests of the inverting flap include the exploration, if possible, of flap deflections which may be used for dive bombing.

With this consideration in mind, a structural design speed of 160MPH has been selected.

The dynamic pressure at this speed is

$$q_{160MPH} = q_{100MPH} \left(\frac{160}{100}\right)^2$$

$$= 65.5 \ \frac{LB}{Feet^2}$$

$q_{120MPH} = 36.9 \ \#/ft^2$

ie $\frac{1}{2}\rho V^2 = \frac{1}{2}(.00238)\left(\frac{150 \times 44}{30}\right)^2 = 65.5 \ \#/ft^2$

The local pressures on the flap can be evaluated numerically with the aid of pressure distributions in this report by the relation

$$P = \frac{P}{q} \ q$$

6. Estimated flap load in pounds per flap and load distributions at 160MPH

6.1 The maximum load, and load distribution, for the attached flow range is,

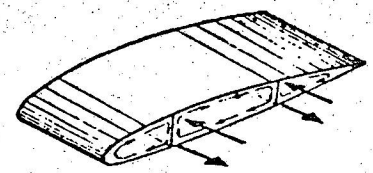

FANASA

FABRICA NACIONAL DE AEROPLANOS S. A.
OFICINA CENTRAL · APARTADO 5599
LIMA · PERU

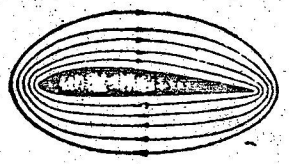

7. Flap loads at 120MPH

It is of interest to determine the flap loads at 120MPH. They are derived from section 6, corrected by the inverse of ratio of the dynamic pressures, which is $\left(\frac{120}{100}\right)^2 = 0.562$

7.1

The flap load for 30° deflection is, from section 6.1,: 1965# (0.562) = 1105 pounds per flap at 120MPH. The resultant force location is not changed.

7.2

The flap load for 90° deflection is, from section 6.2,: 1,300# (0.562) = 731 pounds per flap at 120MPH. The resultant force location is not changed.

8. Special considerations for the inverting flap

For the separated flow regime flap loads have a large steady drag component, and a small varying drag component originating in large-scale turbulence. The magnitude of the varying component is not known, but it could excite flap buffet. Consequently, the flap should be constructed, and supported, taking into account this possibility. A torsion bar or torque tube coincident with the flap hinge line as a method of flap support and actuation is not recommended because of possible torsional oscilations of the flap about the torque tube which could be amplified by the varying drag component. A cable support system as sketched in separate drawings is very satisfactory to provide adequate stiffness to prevent flap buffet for any flap position. The total lack of flap buffet with a properly designed cable system has been verified in test flights.

AAC:rr

Amal | Translation ACS-1

APPENDIX

A. Explanatory footnotes to text of report

(1) It is understood that the difference in crossectional shape will alter the chordwise distribution of the flap load. No attempt has been made to estimate this effect, but the triangular distribution assumed is conservative, as explained in Section 6.1.

(2) When used for flap loads, the influence of flap chord-wing chord ratio, which is small, is being neglected. The flap load used, however, has been calculated on the actual average flap chord, as shown on paragraph 6.1 and 6.2 of this report.

(3) For the sake of speculation a flap load based on 75° deflection and 16° angle of attack will be calculated at 160MPH corrected for 90° deflection, for flap gap, and for chordwise pressure distribution. From the reasoning of subsequent paragraphs, it is, evidently, that determined in 6.2, multiplied by the ratio $\frac{2.1}{1.5}$ from the figures of 4.2. The load is then 1300 (1.4) 1820 pounds per panel. This load would be developed if the aircraft could stall its wing to 16° angle of attack at 90° flap deflection at 160MPH, an obvious imposibility for the aircraft under consideration. That load is, nevertheless, smaller than the 30° flap load calculated at the same speed, which is 1965 LBs from Section 6.1.

B. Symbols

Generally, symbols are those of NACA and NASA conventions. Some symbols frequently used in this report are:

C_f flap chord, (feet)

C wing chord (feet)

δ_f flap deflection, degrees (clockwise positive in drawings measured from rearward projection of wing chord)

section angle of attack (also)

C_l section lift coefficient (also C_{l_o})

C_d section drag coefficient (also C_{d_o})

P pressure, pounds per square foot

q dynamic pressure, pounds per square foot

F force, generalized, pounds

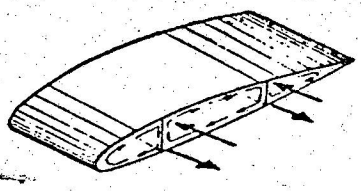

FANASA

FABRICA NACIONAL DE AEROPLANOS S. A.
OFICINA CENTRAL • APARTADO 5599
LIMA - PERU

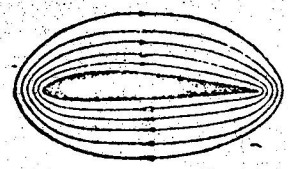

FIG 1

SKETCH OF INVERTING FLAP

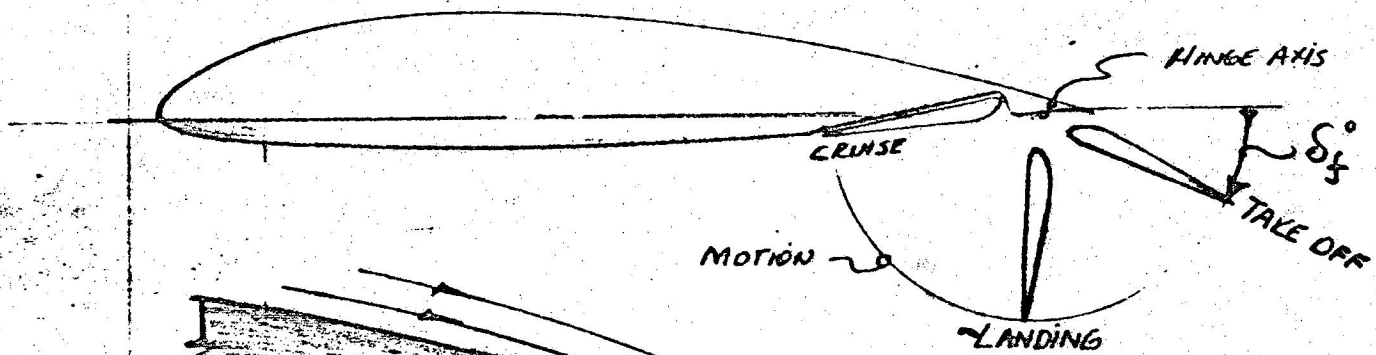

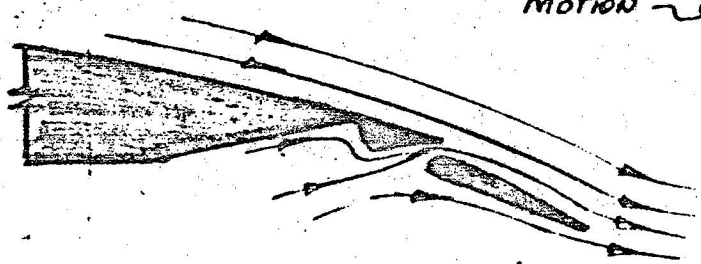

FIG 2A: ATTACHED FLAP FLOW
$10° \leq \delta_f \leq 30°$

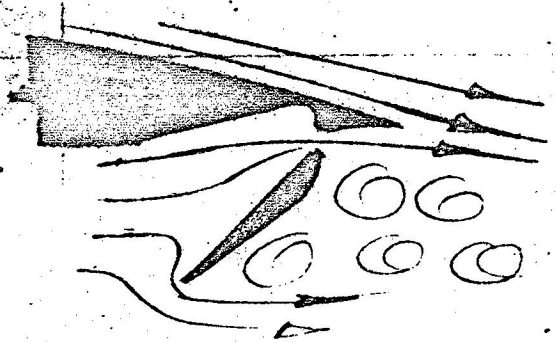

FIG 2C

SEPARATED FLAP FLOW
FLAP INVERTED
$90° < \delta_f \leq 170°$

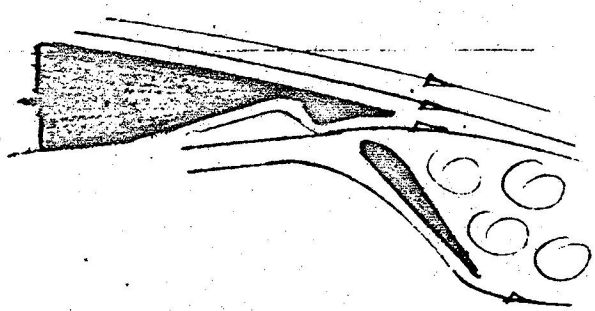

FIG 2B

SEPARATED FLAP FLOW
$30° < \delta_f \leq 90°$

FIG 3

EFFECT OF GAP IN FLAP ON WING DRAG
(REF NACA TN 650 FIG 2, $\alpha = 0$)

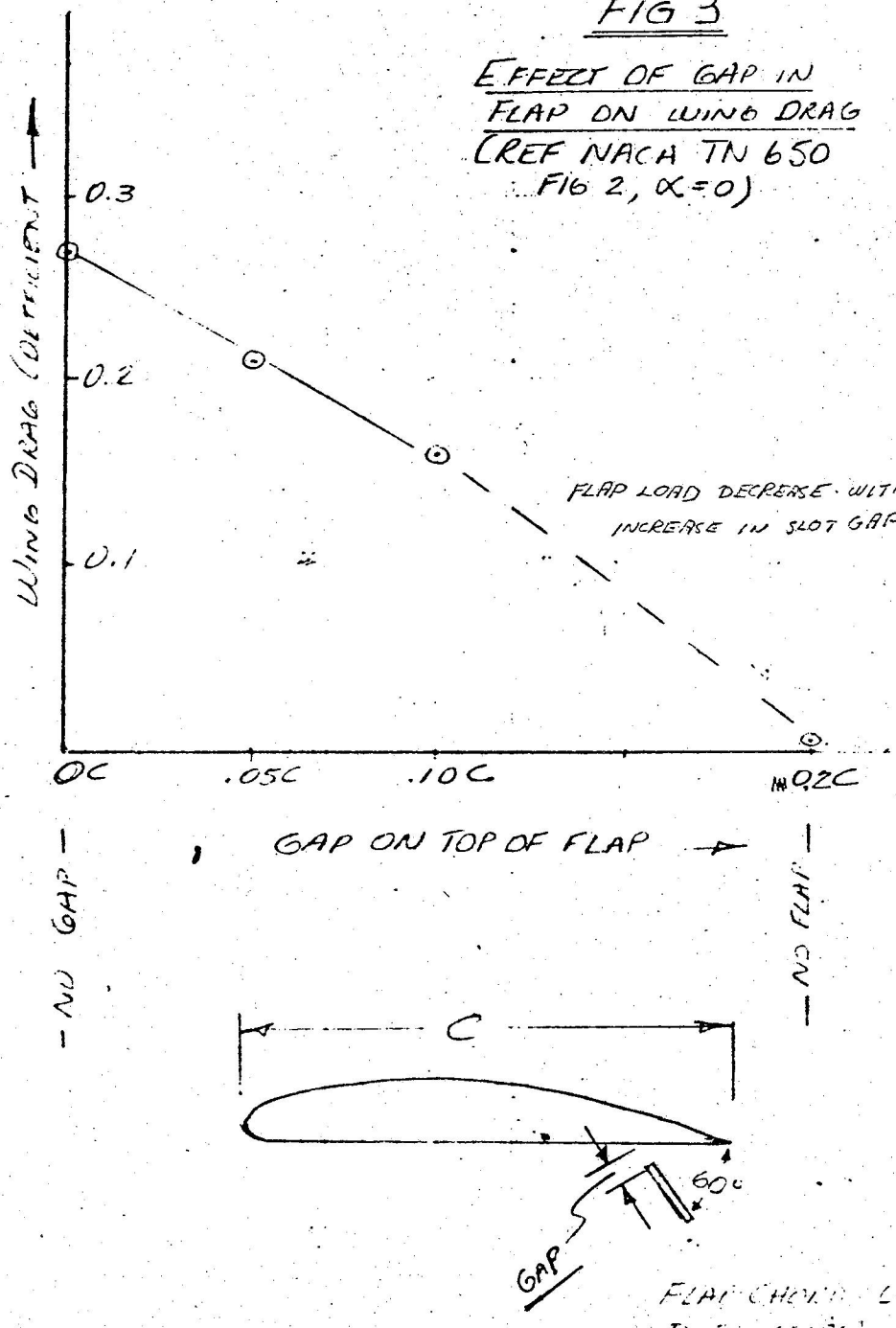

FLAP CHORD 0.20C
DEFLECTION 60°
WING AT α = 0°

FANASA
FABRICA NACIONAL DE AEROPLANOS S. A.
OFICINA CENTRAL • APARTADO 5599
LIMA • PERU

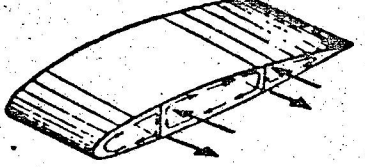

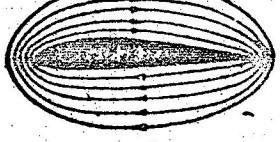

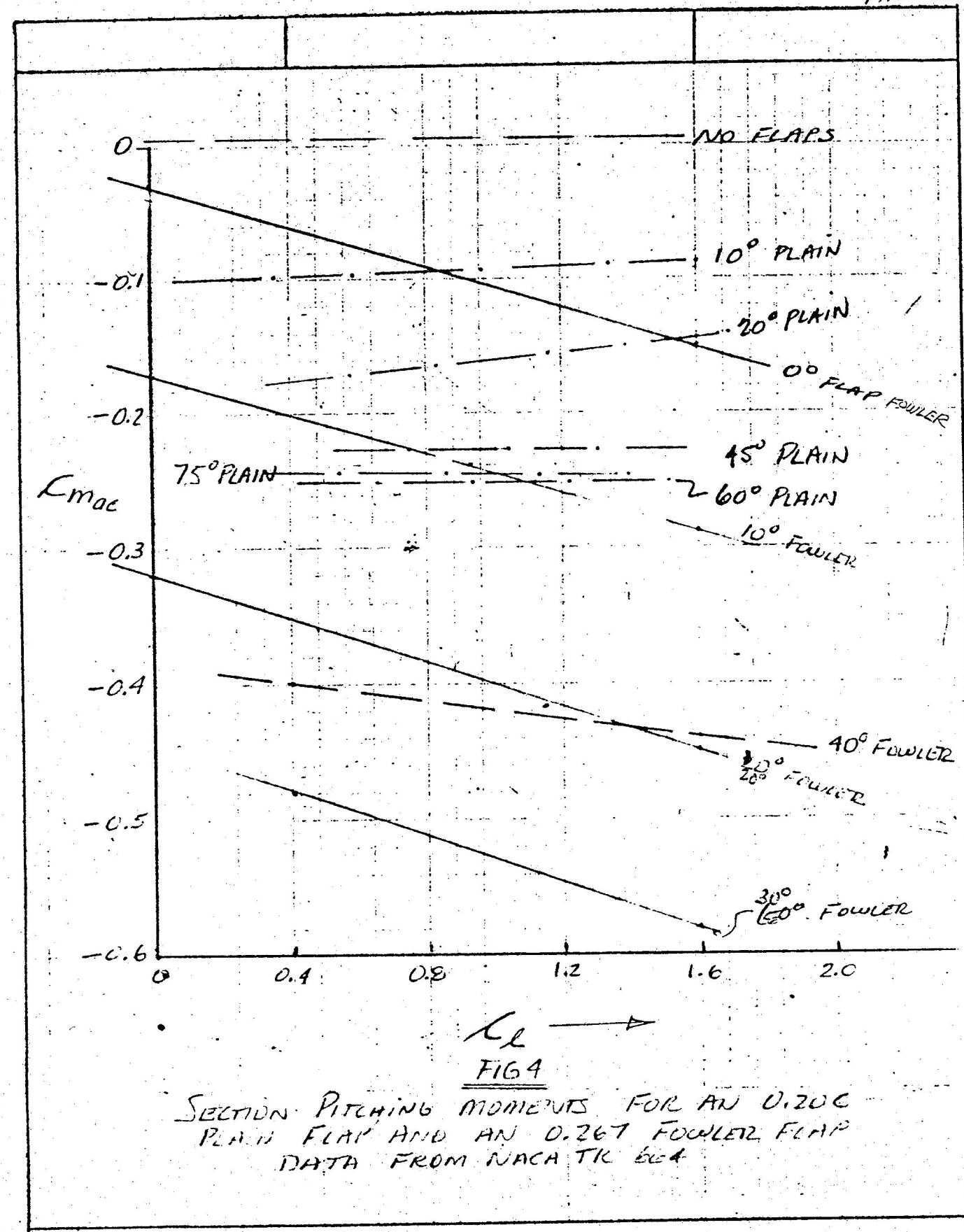

FIG 4

SECTION PITCHING MOMENTS FOR AN 0.20C PLAIN FLAP AND AN 0.26C FOWLER FLAP DATA FROM NACA TR 664

SKETCHES FOR VECTOR REPRESENTATIONS OF PITCHING MOMENT CONTRIBUTIONS

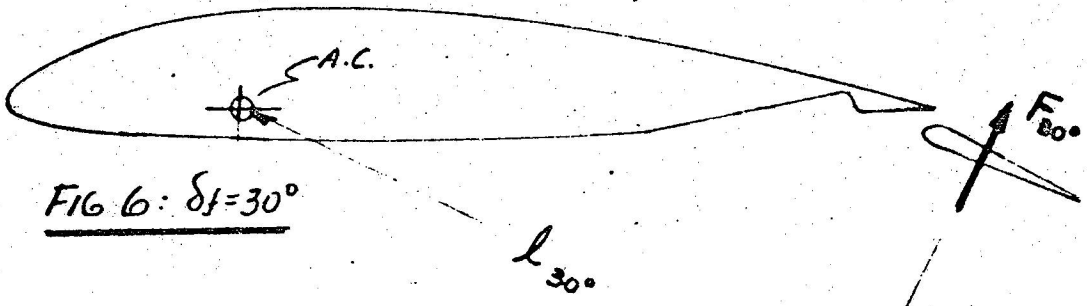

FIG 6: $\delta_f = 30°$

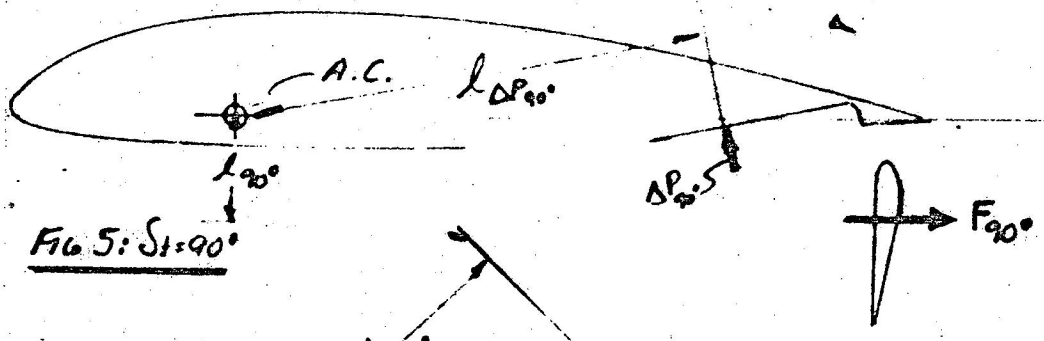

FIG 5: $\delta_f = 90°$

EXPERIMENTAL DATA SHOWS THAT $M_{30°} \gg$ (REF FIG 7)

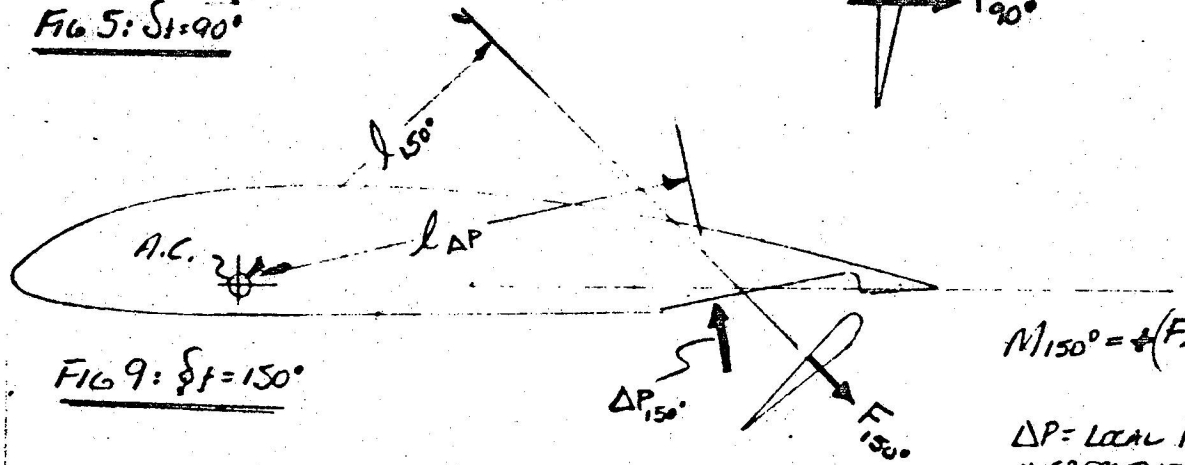

FIG 9: $\delta_f = 150°$

$M_{150°} = +(F\ell)_{150°} - (\Delta$

ΔP = LOCAL PRESSURE INCREMENT ON WING DUE TO FLAP

$F_{30°} > F_{90°} > F_{150°}$

$M \sim F\ell$

$\ell = f(\delta_f)$

$M_{30°} \gg M_{90°} \gg M_{150°}$

FANASA
FABRICA NACIONAL DE AEROPLANOS S. A.
OFICINA CENTRAL - APARTADO 5599
LIMA - PERU

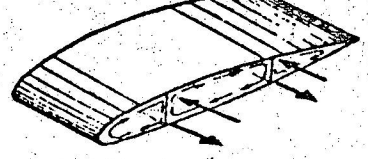

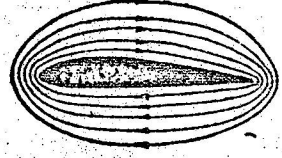

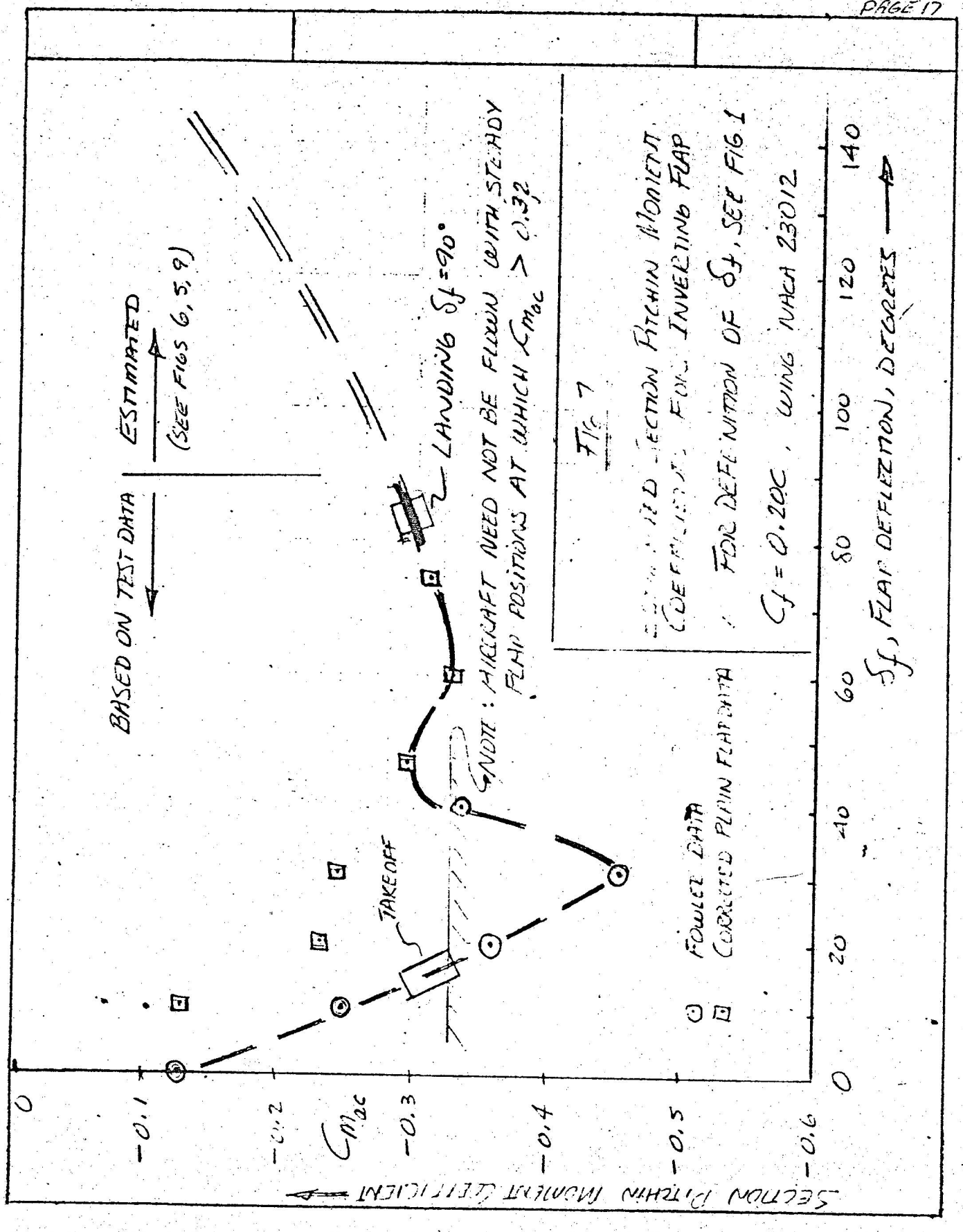

FANASA

FABRICA NACIONAL DE AEROPLANOS S. A.
OFICINA CENTRAL • APARTADO 5599
LIMA • PERU

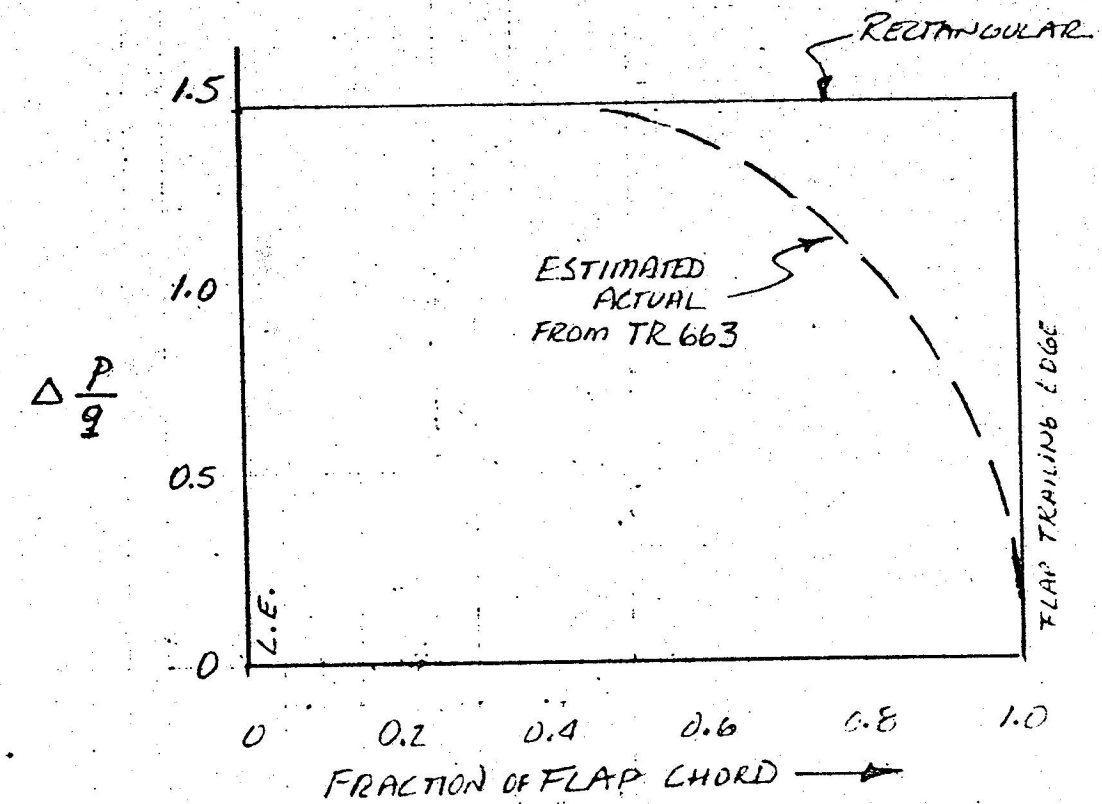

RATIO OF RECTANGULAR AREA TO ACTUAL AREA IS 0.865

FIG 8

ESTIMATED PRESSURE DISTRIBUTION FOR 90° INVERTING FLAP

NOTE: PANEL DATA IS FOR 75° WITH NO SLOT INCREASE OF LOAD DUE TO AIR FLOW DEFLECTION. AND DECREASE DUE TO SLOT, HAVE BEEN TAKEN INTO ACCOUNT IN THE DETERMINATION OF MAXIMUM P_1.

PRESSURE DISTRIBUTION OVER AIRFOILS WITH FOWLER FLAPS

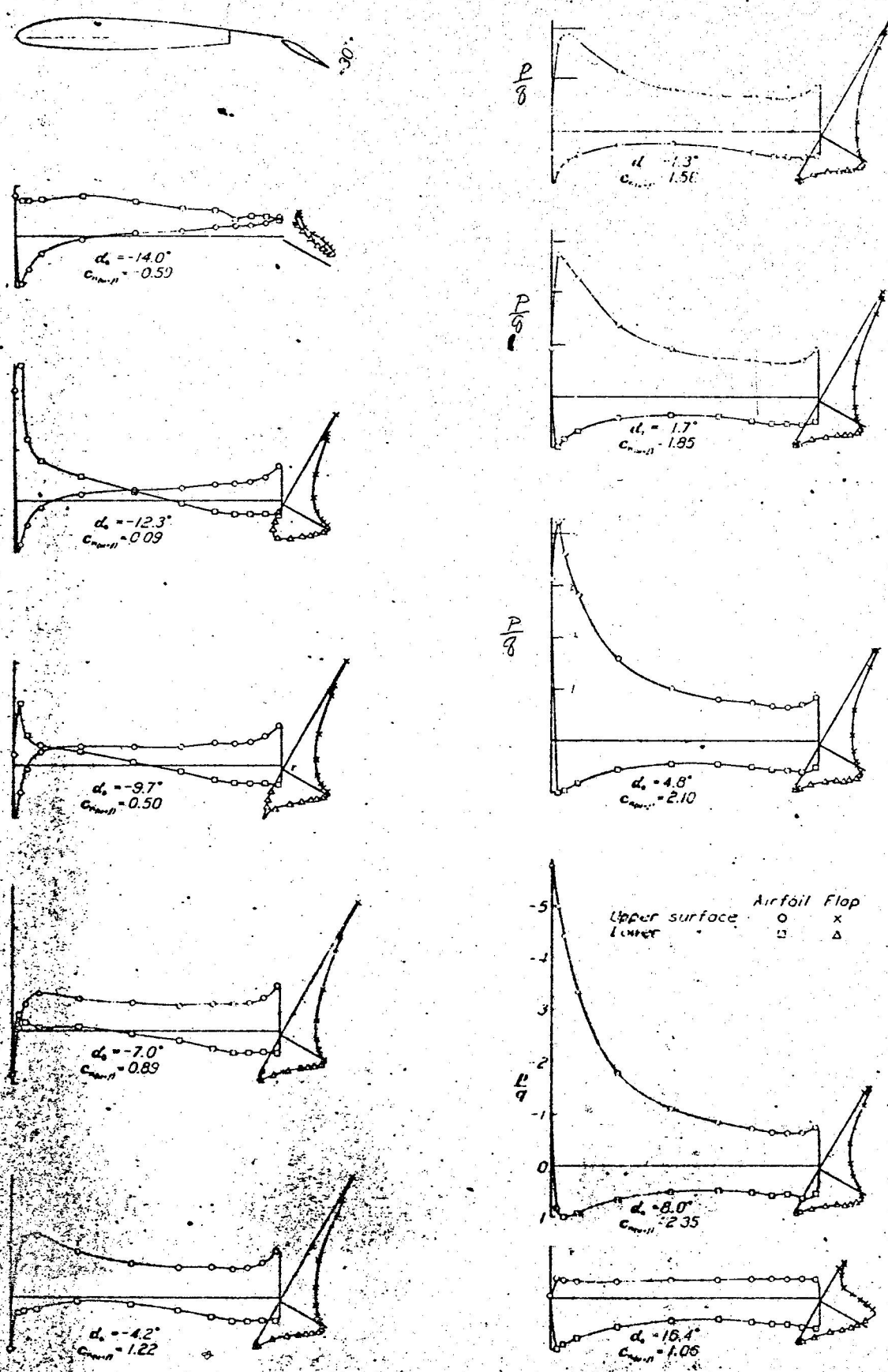

FIGURE 6.—Pressure distribution on the N. A. C. A. 23012 airfoil, with the 0.20c N. A. C. A. 23012 Fowler flap, at various angles of attack. Flap deflected 30°.

PAGE 20

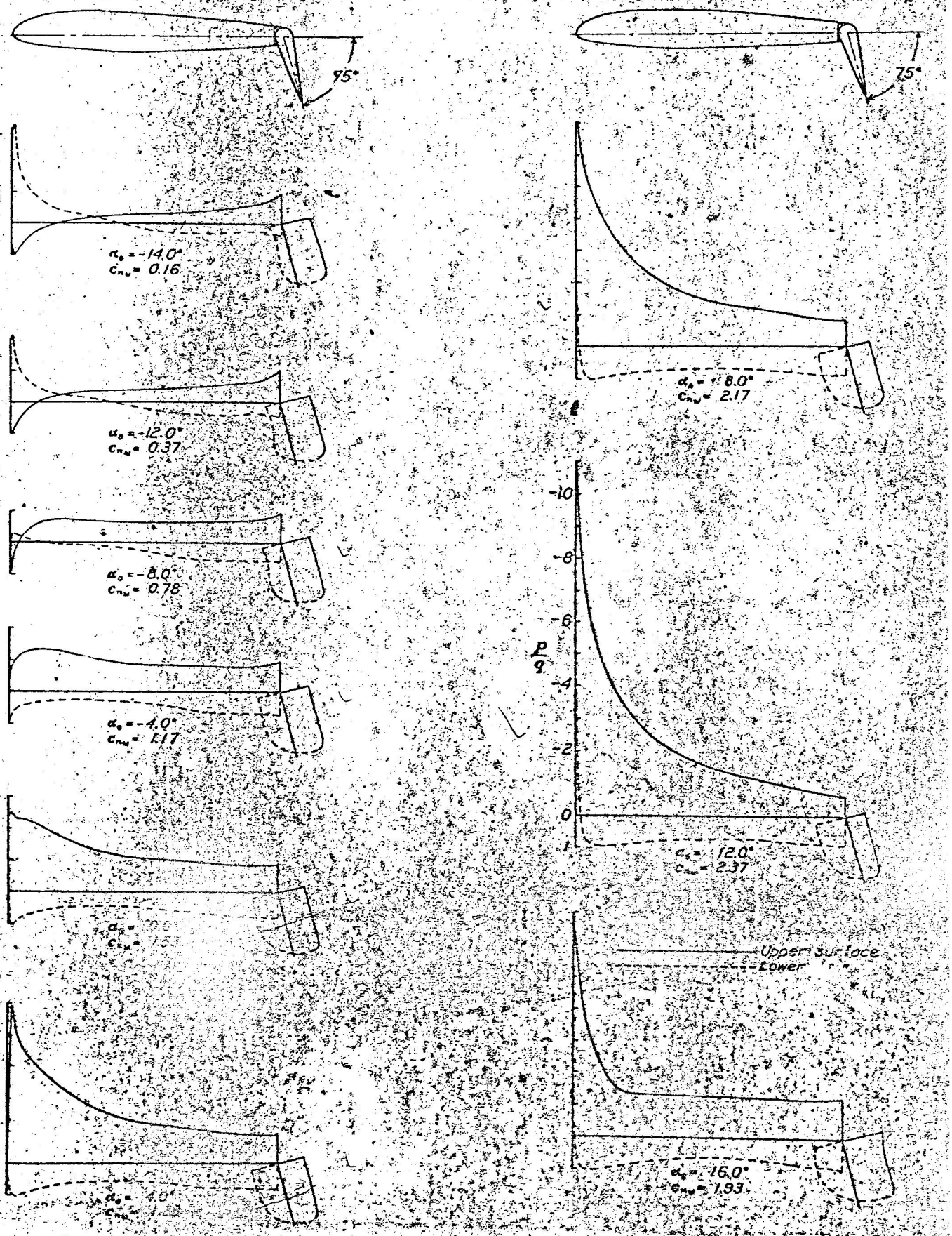

FIGURE 24.—Pressure distribution on the N. A. C. A. 23012 airfoil with a 0.20c plain flap, at various angles of attack. Flap set at 75°.

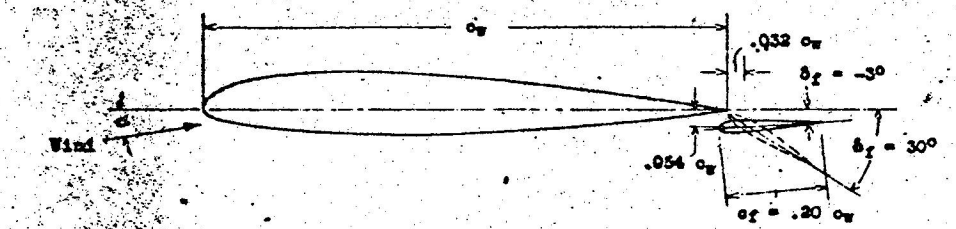

Flap hinge axis 0.25 c_f aft of flap L.E.
0.10 c_f below flap chord

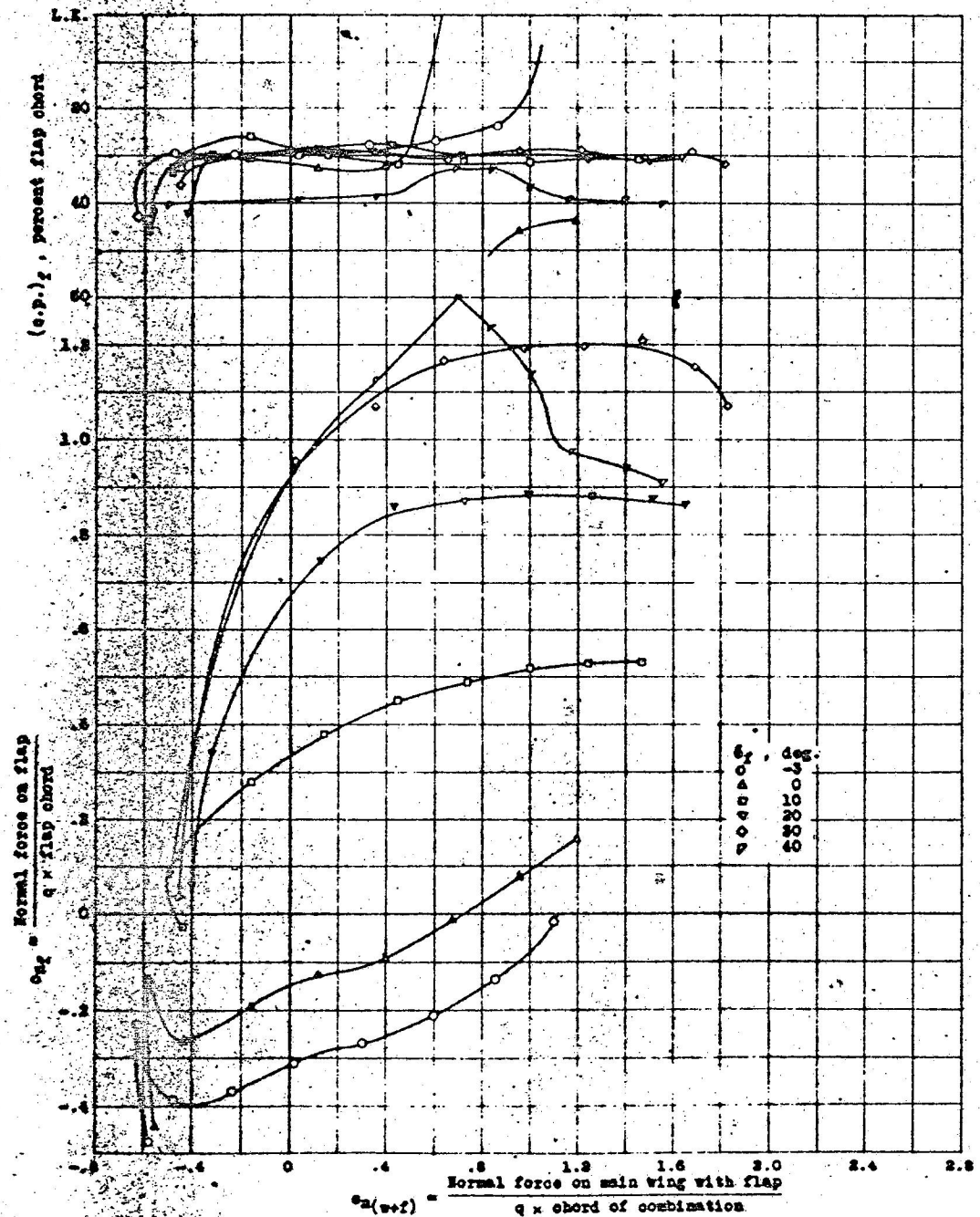

Figure 35.- Normal-force coefficients and centers of pressure of a 0.20 c_w N.A.C.A. 23012 external-airfoil flap on a N.A.C.A. 23012 wing, (reference 15).

PAGE 22

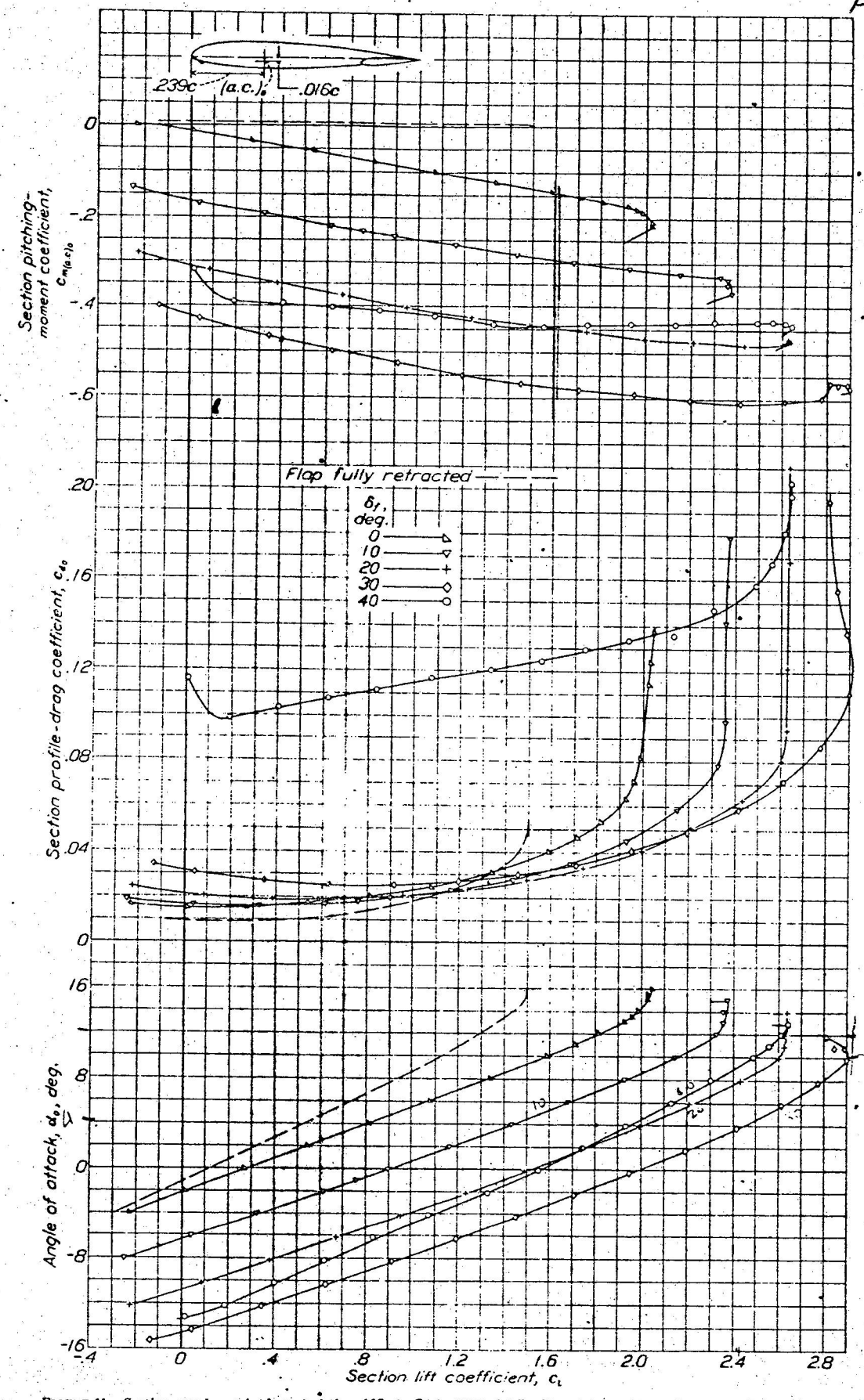

FIGURE 11.—Section aerodynamic characteristics of N. A. C. A. 23012 airfoil with a 0.2667c N. A. C. A. 23012 Fowler flap.

PAGE 23

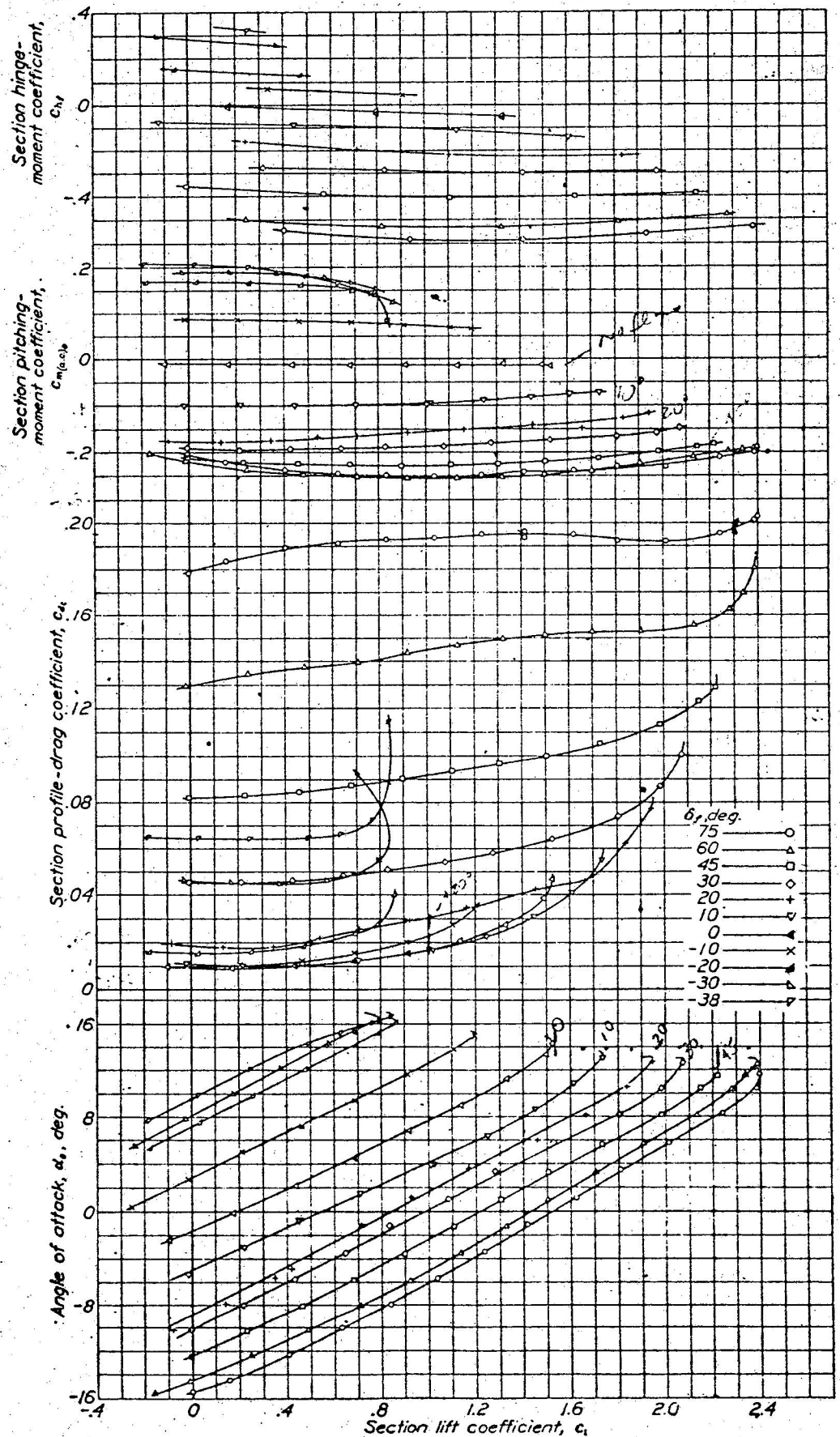

FIGURE 9.—Section aerodynamic characteristics of N. A. C. A. 23012 airfoil with a 0.20c plain flap.

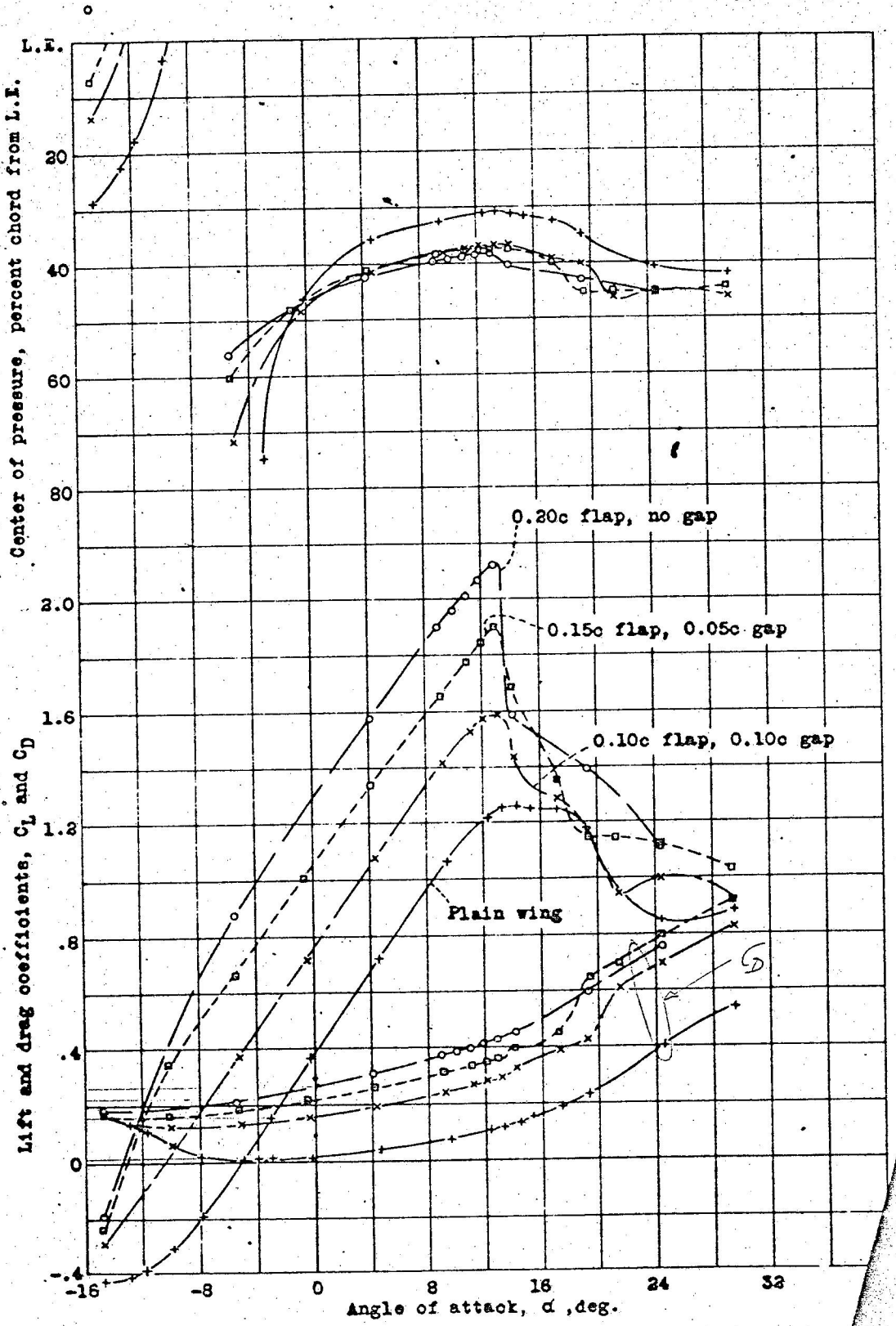

Figure 2.- Lift, drag, and center-of-pressure characteristics of Clark Y wi
full-span split flaps and gap between flap and wing.

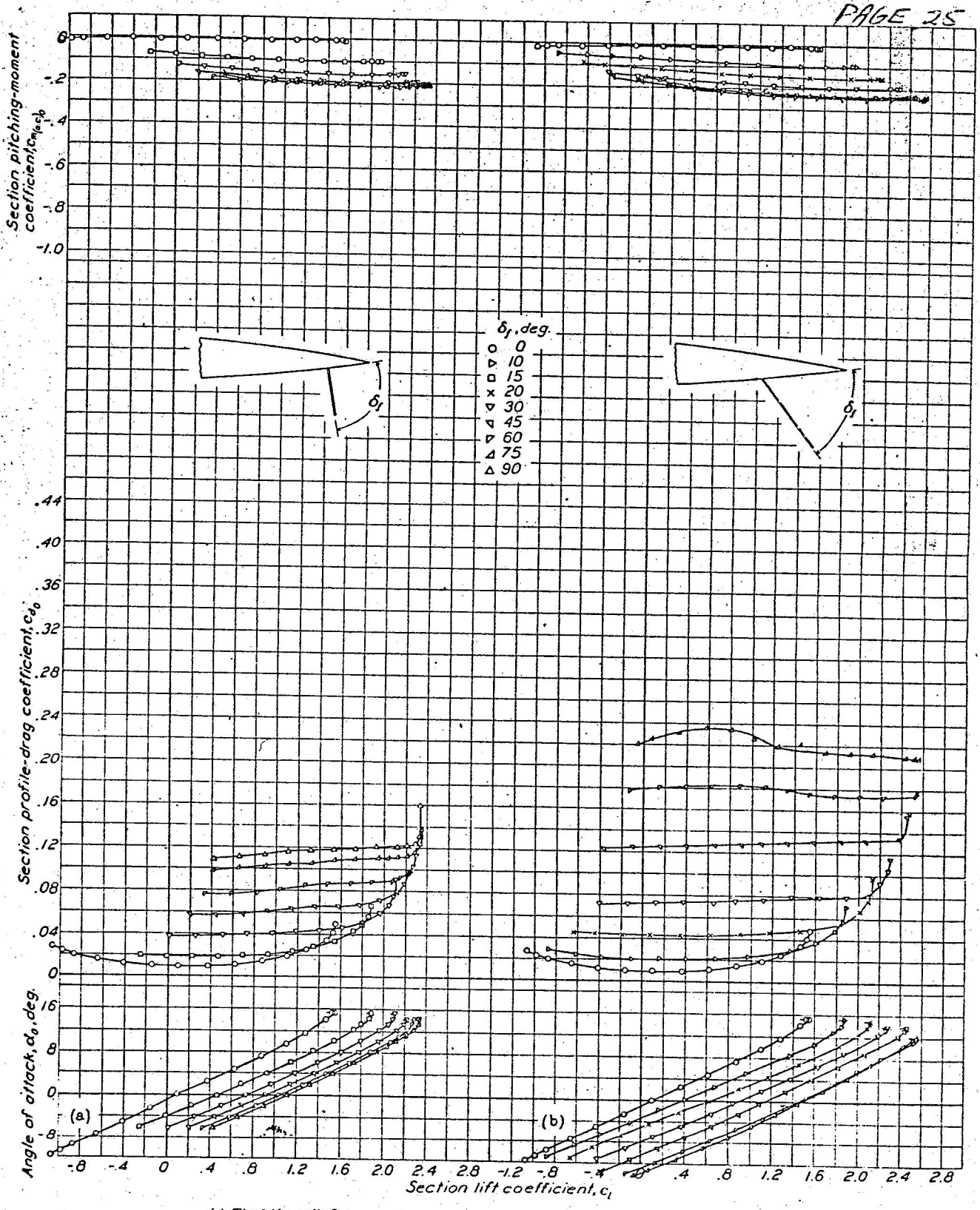

(a) The $0.10c_w$ split flap.

(b) The $0.20c_w$ split flap.

FIGURE 8.—Section aerodynamic characteristics of N. A. C. A. 23012 airfoil with various sizes of split flap.